Minerals Engineering 144 (2019) 106054

Contents lists available at ScienceDirect

Minerals Engineering

journal homepage: www.elsevier.com/locate/mineng

The use of enrichment ratios to support kinetic studies in flotation

L. Vinnett[a,b], G.R. da Silva[c], C. Marion[a], C. Carrasco[b], K.E. Waters[a,*]

[a] Department of Mining and Materials Engineering, McGill University, Montreal, Canada
[b] Departmento de Ingeniería Química y Ambiental, Universidad Técnica Federico Santa María, Valparaíso, Chile
[c] Department of Mining Engineering, Federal University of Minas Gerais, Belo Horizonte, Brazil

ARTICLE INFO

Keywords:
Flotation kinetics
Enrichment ratio
Mineral recovery
Entrainment

ABSTRACT

This paper presents the use and evaluation of enrichment ratios (ER) from different batch flotation protocols. Two protocols under flotation time extensions (> 20 min) are analysed, which favour steady recoveries to be obtained at the end of the process. Agar's criterion is used to evaluate the consistency between the maximum recovery obtained by regression and the total measured recoveries. A good agreement is observed under critical flotation times (t_{crit}) lower than 40% of the total flotation time, where t_{crit} corresponds to the time at which the incremental concentrate grade equals the feed grade (grinding product).

A discretized ER is used as an approximation of instantaneous ER to characterize the evolution of the enrichment along the process. This discrete ER is defined as the ratio between the incremental concentrate grade and the grade of the solid in the flotation cell prior to the respective flotation interval. Discrete ERs greater than 1 along with significant discrete recoveries are feasible, suggesting that further analyses are required to evaluate the process exhaustion. Four size-by-size tests are also studied to assess the distribution of the discrete ERs at long flotation times. Almost all the evaluated classes present discrete ERs greater than 1 in the last flotation intervals. Therefore, the non-selective mechanisms (*i.e.*, entrainment, true flotation of gangue and gangue association) cannot be considered as the predominant contributions to the overall discrete recoveries. Exceptions may be laboratory tests under very fast kinetic responses, high mass recoveries, long flotation times and high content of non-floatable valuable minerals.

1. Introduction

Flotation kinetics allows the comparison of different operating conditions from performance indexes such as recovery rate, concentrate grade, equilibrium recovery, enrichment ratio (ER = Concentrate Grade/Feed Grade) and mass recovery. Kinetic studies are commonly conducted in batch or continuous tests by measuring incremental mass flows as well as concentrate and tailings properties. This information has been typically used to calculate time-recovery, grade-recovery and separability curves, among other possible representations. The enrichment-recovery curves consider the ER along with the process efficiency in the same plot, which have made it possible to compare different flotation schemes under the same levels of selectivity. Agar et al. (1980) incorporated these performance indicators to define a design criterion based on the maximum separability. This analysis considered the flotation separation of fully liberated valuable and non-valuable minerals. A critical flotation time t_{crit} was obtained in the optimal condition, at which the incremental concentrate grade equals the feed grade (raw material to the system). Similar approaches have been reported by other authors, incorporating different descriptions and analysis tools (Jowett, 1975; Maldonado et al., 2011; Seguel et al., 2015). All these approaches assume that after a critical flotation time, the recovery of non-valuables becomes significant and the economics of the process are negatively impacted.

Several studies have highlighted the predominant non-selective behaviour at the end of the flotation process. For example, Sutherland (1989) used QEM*SEM (Quantitative Evaluation of Minerals by Scanning Electron Microscopy) analysis to evaluate batch flotation kinetics of composite particles. The flotation tests were performed in a 2.7 L laboratory cell and the resulting time-recovery curves were modelled by two rate constants (Kelsall, 1961). The flotation rates of the slower components were considered comparable to the recovery rates by entrainment. Ross (1990) reported a methodology to separate the effect of true flotation and entrainment in flotation. Entrainment was assumed to be the only mechanism for solid recovery at $t \rightarrow \infty$. Girard et al. (2005) presented simulated kinetic responses with very slow rates after six minutes, attributed to entrainment of slow floating particles rather than true flotation. Runge (2010) reported different techniques to interpret laboratory flotation results, and a methodology to determine the

* Corresponding author.
E-mail address: Kristian.Waters@McGill.ca (K.E. Waters).

https://doi.org/10.1016/j.mineng.2019.106054
Received 7 December 2018; Received in revised form 2 August 2019; Accepted 26 September 2019

concentrate flow of a component due to entrainment. A classification or drainage function was estimated, assuming that towards the end of a flotation test, the predominant recovery mechanism was entrainment. Ramlall (2013) and Ramlall and Loveday (2015) used kinetic and entrainment models to separate the effect of the selective and non-selective processes in flotation. Both mechanisms were directly estimated by non-linear regression. The non-selective component represented the prevailing process to recover valuable minerals at long flotation times.

Non-selective recovery mechanisms typically represent the most significant contribution for the recovery of overall solids later in the flotation processes. However, industrial data has shown that enrichment may still be obtained by the end of a flotation stage. Examples of mass balances along industrial flotation circuits have been reported by Celik (2015), Hay (2008), Savassi (2006), Yianatos et al. (2006), Zanin et al. (2009), among others. From these studies, a comparison between the concentrate and tailings grades (or feed if available) in the last cell of the circuits leads to estimated ERs in the range of 3–15. Hadler (2015) related the grades of the attached particles at the froth surface (lamellae grades) with the feed grades in the first four cells of an industrial rougher bank. The lamellae grades were considered the highest achievable grades, given the properties of the feed to the flotation machine. A non-linear trend between the normalized lamellae grades and the normalized cell feed grades was obtained. Thus, the properties of the froth surface were defined by the characteristics of the feed material. Yianatos et al. (2014) and Yianatos et al. (2016) measured the top-of-froth (TOF) grades cell-by-cell in two different rougher flotation banks. As with the lamellae samples, the TOF grades also present lower sensitivity to entrainment compared to the concentrate streams, allowing the potential grades in the last cells to be estimated. These TOF grades in the last cells were in the range of 1.5–3.8% Cu for the studied banks, which was approximately 2.5–4.5 times the circuit feed grades.

The information provided above presents two different points of view for the flotation behaviour under long flotation times. Mineral exhaustion has been typically determined by kinetic studies in flotation. Garcia-Zuñiga (1935) reported the first time-recovery characterization at batch scale, using the expression $R(t) = R_\infty \cdot (1 - e^{-kt})$ for modelling purposes. In this expression, k corresponds to the flotation rate constant, t the flotation time and R_∞ the maximum or equilibrium recovery. The parameter R_∞ was defined as the maximum amount of valuable mineral that can be recovered under specific experimental conditions. Similar definitions for R_∞ have been used in literature, implying that a flotation time longer than a defined limit does not lead to further improvement in process efficiency (Agante et al., 2007; King, 2012; Trahar and Warren, 1976). The total flotation time in laboratory tests is typically set based on froth characteristics (*e.g.* barren froth), by comparison with an industrial flotation time (given a scale-up factor) or to standardize the flotation protocols using typical time-recovery trends. The selectivity is, however, rarely reported in kinetic studies or is presented relative to the initial feed grade, ignoring enrichment throughout the flotation process.

This paper presents the use of enrichment ratios to analyse six batch flotation processes with different protocols and levels of selectivity. Three aspects were studied: (i) the consistency between the R_∞ values obtained by regression with the total measured recoveries, under a wide range of t_{crit} values obtained from Agar's criterion; (ii) the enrichment and recoveries at long flotation times to evaluate the level of exhaustion in the evaluated flotation processes; (iii) the distribution of the ERs in different size classes to infer the potential contribution of true flotation to the recovery of valuable metals at the end of the tests. The analysis can be used to complement the information provided from kinetic studies.

2. Methodology

2.1. Flotation tests

Six batch datasets were studied to characterize the ERs along the flotation process. Each flotation test (namely Test A to F) considered different ores, laboratory protocols and mass recoveries. Tests A, B and C correspond to the rougher separation of copper minerals from different gangue, Test D to the rougher separation of copper-lead from a complex ore (Pb-Cu-Zn) and Tests E and F to the rougher separation of sulphides from silicates. Each ore presented different mineralogy and grain sizes, which imposed specific constraints to the feed particle size. Tests A and B involved the flotation of different samples from two mine sites (55 and 85 samples for Tests A and B, respectively). Tests A and B were studied for unscreened concentrate and tailings products, whereas Tests C to F were also analysed size-by-size. The size-by-size tests included replicates and/or the evaluation of different operating conditions, according to the material availability. The size classes were defined based on the particle size distribution of the feed solid. The ores were initially crushed and wet ground to obtain the required particle sizes. The pulps were then poured into the flotation cells for conditioning and flotation. Lime was used as a pH regulator in all cases and make-up water (at the operating pH) was used to adjust the pulp level. Manual scraping was conducted in all the evaluated datasets. In Tests A and B, the scraping frequency was adjusted at a rate of one every 5 s for the three first minutes, followed by once every 15 s. In Test C, the scraping rate was set at one every 10 s along the whole experiment. In Tests D to F, the scraping was set at an approximate rate of one every 1 s (fast scraping rate). In all cases, the finest class of the studied products was wet screened (*e.g.* at 20 μm, 38 μm or 45 μm) and the oversize was dry screened by sieve shaking. Test E required for the combination of the products from two runs to increase the mass of the incremental concentrates. Tests A, B and D included extended flotation times (longer than 16 min) to enhance the ultimate recovery estimations. In Tests E and F, the same ore was processed with different grinding schemes, flotation times, initial masses, size classes, solid percentages and frother concentrations. In Test F, the grinding process was set to guarantee 100% passing 106 μm in the flotation tests (Mohammadi-Jam, 2017). Tables 1 and 2 detail the main aspects of each flotation protocol and mineral characteristics, including: composition of the main valuable minerals and gangues, initial masses, particle sizes (P_{80}), solid percentages, feed grades, analysed size classes, cell volumes, superficial gas rates (J_G), pH, reagent types and concentrations, impeller speed and flotation times. The footnote of Table 1 presents some previous studies that can be consulted for further details on the experimental procedures.

Table 3 shows the mass recoveries, overall ERs (total concentrate grade/ feed grade) and metal recoveries in the evaluated datasets. These indexes showed wide ranges in Tests A and B (unscreened tests). Based on the median, Test B presented lower recoveries and higher overall ERs compared to Test A, as shown in the cumulative distribution functions (CDF) of Fig. 1. Tests C to F (size-by-size tests) presented different levels of selectivity with overall ERs in the range of 1.6 to 6.2. Fig. 2 illustrates the size-by-size kinetic responses in Tests D (lead) and E (nickel), which showed significant differences in the mass recoveries (24% and 55%, respectively). Slower flotation kinetics are observed in the fine classes compared to the intermediate classes; however, slightly higher potential recoveries can be estimated in the former case due to the increasing trends in the last flotation intervals. Lower ultimate recoveries were typically obtained in the coarse class. Appendix A shows examples of flotation kinetics in Tests C and F.

2.2. Data analysis

To complement the information obtained from the kinetic studies, the following analyses are proposed: (i) comparison between the total measured recoveries and the R_∞ values obtained by regression, at different critical flotation times obtained from Agar's criterion; (ii) estimation of discrete ERs and discrete recoveries (as approximations for the instantaneous indexes) at long flotation times to assess the process efficiency under exhaustion; (iii) estimation of the discrete ER in different size classes to infer the potential contribution of true flotation (or

Table 1
Feed characteristics, number of datasets and size classes in the batch flotation tests.

Test	Valuable Minerals	Main Gangues	Initial Mass (kg)	P_{80}, μm	Feed Grades, %	No of Conditions	No of Repetitions per Condition
A	Chalcocite, Enargite	Silicates, Pyrite	1.3	212	0.6–2.3 Cu	55	0
B[(1)]	Chalcopyrite, Chalcocite, Covellite	Silicates, Clays, Pyrite	0.75	150	0.3–1.2 Cu	85	0
C[(2)]	Chalcopyrite, Bornite	Pyrite, Silicates	1.6	150	0.8–1.0 Cu	2	2 and 1, respectively
D	Galena, Chalcopyrite	Pyrite, Sphalerite, Silicates	0.5	53, 75	2.5–2.7 Pb, 0.9–1.0 Cu	3	2, 1 and 0, respectively
E[(3)]	Chalcopyrite, Pentlandite, Pyrrhotite	Silicates	0.4	75, 106, 150	1.4 Ni, 1.0–1.1 Cu	3	2
F[(3)]	Chalcopyrite, Pentlandite, Pyrrhotite	Silicates	0.5	63	1.4 Ni, 1.0–1.1 Cu	1	2

(1) Vinnett et al. (2019).
(2) Carrasco (2010).
(3) Mohammadi-Jam (2017).

Table 2
Operating conditions in the batch flotation tests.

Test	Cell Type/Volume, L	Solid Percentage, %	J_G, cm/s	pH	Reagent Types and Concentrations	Impeller Speed, rpm	Flotation Times, min Size Classes, μm
A	Denver, 2.7	33	0.52	10.3	Collectors: Aero 473 Promoter (40 g/t) Sodium Isopropyl Xanthate (15 g/t) Frother: Flotanol H70 (20 ppm)	1000	1, 3, 5, 8, 12, 16, 20 No size-by-size analyses
B	Denver, 2.0	30	0.46	10.0	Collectors: Modified dithionocarbamate (33 g/t) Modified sodium di-isobuthyl-dithiosulfate (11 g/t) Frother: Complex oxygenate/hydrocarbon mixture (11 ppm)	1100	1, 3, 6, 10, 15, 20, 25, 30 No size-by-size analyses
C	Wemco, 2.6	43	0.88	9.5	Collectors: Blend NP-107/D-101 (50–50, 31 g/t) Xanthate AX-343 (11 g/t) Frother: Flomin-810 (4.5 ppm)	1440	1.5, 3, 6, 12 −45, +45–150, +150
D	Denver, 1.5	30	0.55	9.3	Collector: Aerophine 3418A (40 g/t) Frother: MIBC (24 ppm) Depressant: Sodium Metabisulfite (1500 g/t)	1200	0.33, 1, 4.5, 10, 16, 24, 32 −20, +20–38, +38
E	Denver, 1.5	25	0.47	9.5	Collector: Potassium Amyl Xanthate (140 g/t) Frother: Dowfroth 250C (25 ppm)	1200	0.5, 1, 4, 8, 16 −38, +38–75, +75–150, +150
F	Denver, 1.5	30	0.47	9.5	Collector: Potassium Amyl Xanthate (140 g/t) Frother: Dowfroth 250C (75 ppm)	1200	0.5, 1.5, 3.5, 7.5 −38, +38–75, +75–106

non-selective processes) to the recovery at the end of the tests. For further details about the enrichment ratios, refer to Appendix B.

2.3. Comparison between R_∞ and measured recoveries: Use of Agar's criterion

Agar's criterion was used to compare the maximum recoveries obtained by regression with the total measured recoveries at the end of the tests. This criterion defines the flotation time at which the optimal separation of two liberated minerals is achieved. This critical time t_{crit} is obtained when the incremental concentrate grade equals the feed grade to the system (Agar et al., 1980). Equivalently, t_{crit} is obtained when the incremental ER equals 1. From this t_{crit}, the incremental concentrates generally have lower quality than the initial feed.

Table 3
Mass recoveries, overall ERs and recoveries in Tests A to F.

Tests	Mass Recovery, %	Overall Enrichment Ratio	Recovery, %
A	18% − 33%	Cu: 2.8–5.2	Cu: 85% − 97%
B	8% − 30%	Cu: 3.2–11.1	Cu: 82% − 97%
C	18% − 23%	Cu: 4.6–6.2	Cu: 90% − 91%
D	17% − 24%	Pb: 3.4–4.5 Cu: 3.7–5.0	Pb: 77% − 83% Cu: 84% − 91%
E	55% − 59%	Ni: 1.6–1.7 Cu: 1.6–1.7	Ni: 89% − 96% Cu: 89% − 96%
F	55%	Ni: 1.6 Cu: 1.8	Ni: 86% − 87% Cu: 98%

The incremental recoveries for flotation times longer than t_{crit} are the product between an incremental ER (< 1) and the incremental mass recovery. As the incremental ER and mass recovery typically decrease as flotation time increases, the asymptotic behaviour of the flotation kinetics is approached for $t > t_{crit}$.

The incremental ERs were plotted as a function of time and the t_{crit} values were obtained by piecewise cubic Hermite interpolation (The MathWorks, USA). The ratio between the critical time and the total flotation time t_{crit}/t_{tot} was then used as a reference parameter. A Gamma distribution was utilised to describe the flotation rate distribution $F(k)$ due to its flexibility and low number of parameters (Harris and Chakravarti, 1970; Imaizumi and Inoue, 1963; Vinnett et al., 2015). Table 4 shows the expressions for $F(k)$ and for the cumulative recovery $R(t)$ in batch flotation. The maximum recovery and $F(k)$ parameters were determined by least-squares estimation (Vinnett et al., 2015). Fig. 3 illustrates the model fitting for a time-recovery curve. The relative differences between the total measured recoveries $R(t_{tot})$ and the estimated R_∞ values were analysed for different ranges of t_{crit}/t_{tot}.

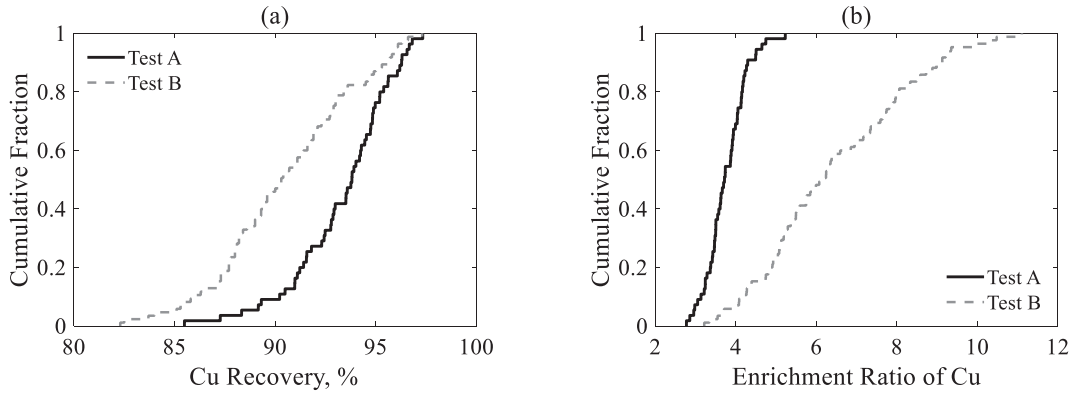

Fig. 1. Comparison of metallurgical indexes between Tests A and B, (a) Cu recoveries, (b) Enrichment ratios of Cu.

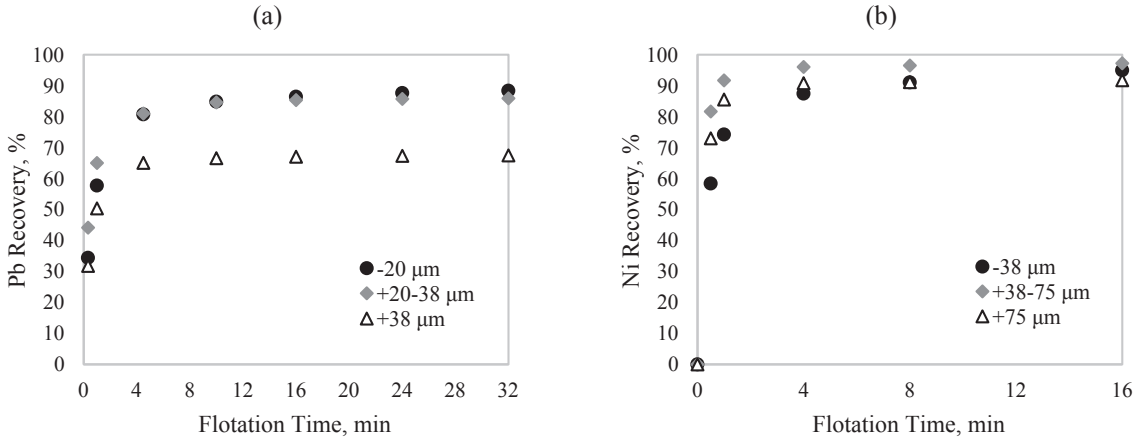

Fig. 2. Recovery as a function of time for different size classes: (a) Pb kinetics, Test D, P_{80} = 53 μm; (b) Ni kinetics, Test E, P_{80} = 106 μm.

Table 4
Expressions for $F(k)$ and $R(t)$ in a batch flotation process.

	Expressions	*Parameters*
Flotation Rate Distribution	$F(k) = \frac{k^{a-1}}{k_0^a \cdot \Gamma(a)} \cdot \exp(-k/k_0)$	a: shape parameter k_0: scale parameter Γ: Gamma function t: Flotation time R_∞: Maximum recovery
Recovery of a Batch Process	$R(t) = R_\infty \cdot \left[1 - \frac{1}{(1+k_0 \cdot t)^a}\right]$	

2.4. Estimation of discrete ERs and discrete recoveries at long flotation times

The discrete ERs along with the discrete recoveries were also studied for long flotation times. The discrete ERs were obtained from mass balances, using the grades and solid weights of the tailings and concentrates. This procedure made it possible for the back-calculation of the grades and weights of the solid that was in the flotation cell before the concentrate removal. The mass balance was iteratively applied to all the flotation intervals to account for the evolution of the discrete ERs and recoveries as a function of time.

2.5. Distribution of the discrete ERs size-by-size

The same back-calculation procedure was applied to size-by-size tests, according to their availability. The size-by-size analyses allowed typical distributions of the discrete ER to be observed as a function of particle size. These distributions made it possible to infer the potential contributions of the different recovery mechanisms for valuable metals at the end of the flotation tests.

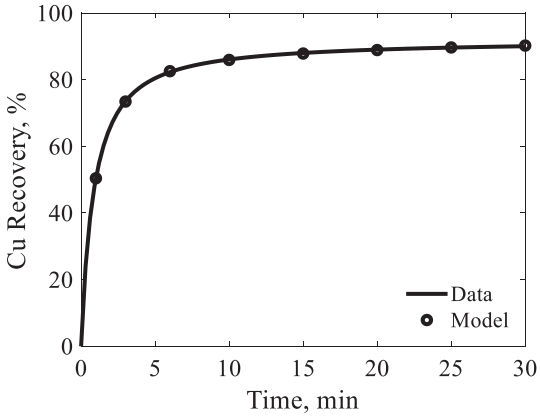

Fig. 3. Example of a time-recovery curve and model fitting assuming a Gamma $F(k)$.

3. Results and discussions

3.1. Comparison between R_∞ and measured recoveries: Use of Agar's criterion

The unscreened Tests A and B were used to evaluate the consistency in the estimation of potential recoveries. These tests presented long flotation times and a high number of runs, which was suitable to obtain

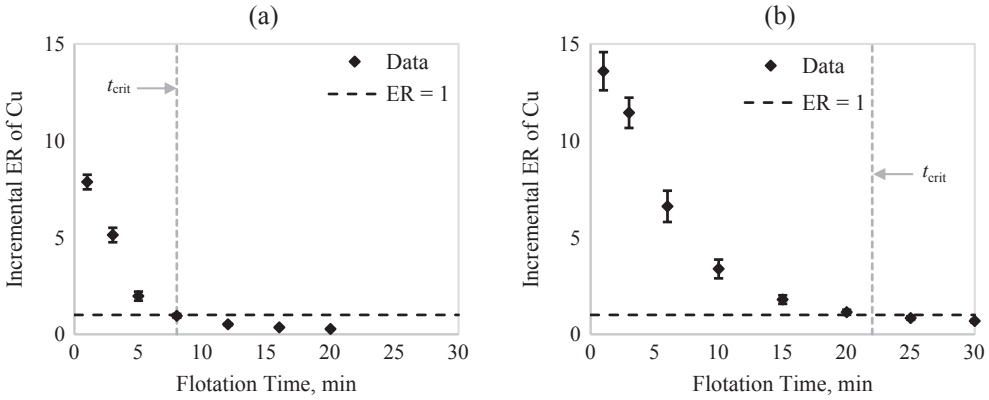

Fig. 4. Incremental enrichment ratios: (a) Test A; (b) Test B.

a representative database. Fig. 4a and b show the mean values for the incremental ERs in Tests A and B, respectively. The 95% confidence intervals of the mean are also displayed. An incremental ER of 1 corresponds to the critical condition defined by Agar's criterion. The critical flotation times were obtained at approximately 8 and 22 min for Test A and B, respectively. All the conditions in Test A reached an incremental ER = 1 in the 20 min of flotation; however, 20% of the conditions in Test B did not fulfil the Agar's criterion. The flotation protocol of Test B showed higher selectivity, which is in good agreement with the results presented in Fig. 1.

The relative difference between the estimated R_∞ values and the total measured recoveries were evaluated for Tests A and B (at t_{tot} = 20 min and t_{tot} = 30 min, respectively). Fig. 5 shows the cumulative distribution functions for $|R(t_{tot}) - R_\infty|/R(t_{tot})$. The R_∞ values were obtained by model fitting. The CDFs were grouped into three ranges of t_{crit}/t_{tot}. For $t_{crit}/t_{tot} < 0.4$, lower differences between the total measured and the estimated maximum recoveries were observed. These differences were significantly higher for $t_{crit}/t_{tot} \geq 0.4$. Experiments with $t_{crit}/t_{tot} \geq 0.7$ presented differences higher than 10%, as shown in Fig. 5b. Therefore, for high t_{crit}/t_{tot} values, the R_∞ values obtained by regression can be significantly different to the measured recoveries at the end of the tests.

Fig. 5 shows that the R_∞ values were more consistent with the total measured recoveries for lower t_{crit}/t_{tot} ratios, suggesting that these ratios can be used to define appropriate flotation times for batch tests. From Fig. 5, flotation times should be between 2 and 3 times the t_{crit} obtained from Agar's criterion to obtain more accurate estimates for potential recoveries.

The flotation kinetics of Tests A and B were obtained from moderate low-grade ores and batch tests subject to selectivity constraints. Other systems may present deviations regarding the results observed in Fig. 5. For example, ores with a very high concentration of valuable minerals in the ultrafine fractions may not reach the asymptotic behaviour even for $t_{tot} \gg t_{crit}$.

3.2. Estimation of discrete ERs and discrete recoveries at long flotation times

The discrete enrichment ratios were also studied for Tests A and B. Fig. 6 shows these ratios together with the discrete recoveries of Cu (labelled in Fig. 6) along the process. Both indexes were estimated regarding the material kept in the cell at the beginning of the respective interval. The 95% confidence intervals of the mean are again presented. The discrete ERs were not negligible at the end of the process with mean values of 2.8 ± 0.2 and 6.0 ± 0.5 in Tests A and B, respectively. The discrete recoveries at the end of the experiments were lower than 10% in longer time intervals. However, these values were calculated under the assumption that all the valuable metal can be recovered (*i.e.* R_∞ = 100%). The maximum recovery is a parameter that dynamically changes along the flotation process according to $R_\infty(t) = (R_\infty(0) - R(t))/(1 - R(t))$. For example, for an initial $R_\infty(0)$ = 95% and a total recovery of $R(t_{tot})$ = 90%, the final maximum recovery is $R_\infty(t_{tot})$ = 50%. Thus, the last discrete recovery, normalized by the maximum recoverable metal $R(t_{tot})/R_\infty(t_{tot})$, may be significantly higher than the measured value when $R_\infty(0)$ is close to $R(t_{tot})$.

Although entrainment critically influences the mass recovery as the valuable minerals become exhausted, the discrete ERs at the end of Tests A and B (2.8 and 6.0) suggest a significant effect of the selective processes on the overall discrete recoveries.

3.3. Distribution of the discrete ERs size-by-size

The size-by-size tests allowed the distribution of the discrete ERs to

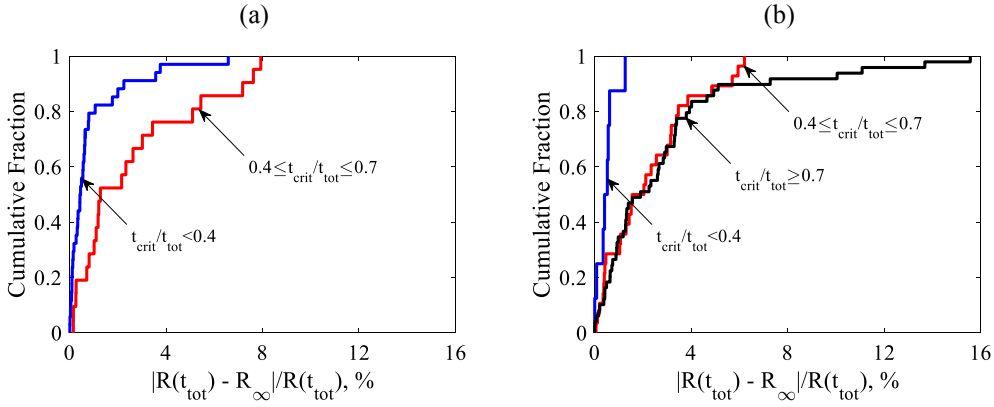

Fig. 5. Cumulative distribution functions of the relative difference between the R_∞ values and the total recoveries for different t_{crit}/t_{tot} ratios: (a) Test A; (b) Test B.

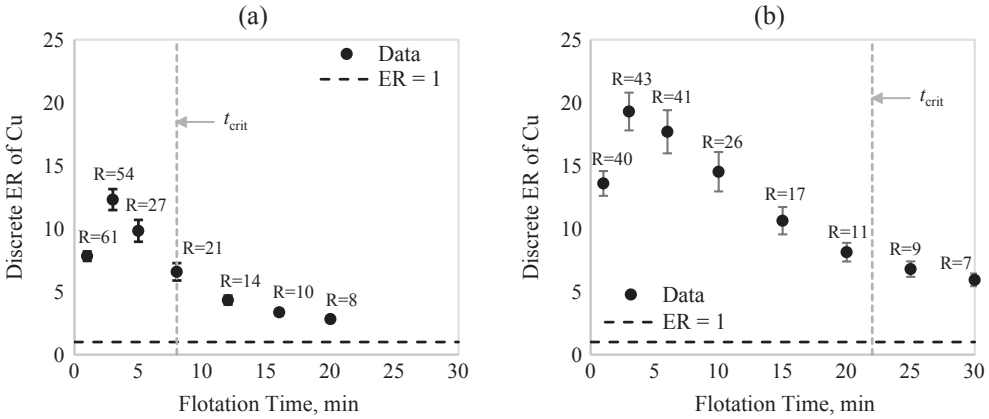

Fig. 6. Discrete enrichment ratios of Cu along with the discrete Cu recoveries (data labels): (a) Test A; (b) Test B.

be evaluated under different flotation protocols and levels of selectivity. Tests C to F presented the decreasing or similar trends to those observed in Figs. 4 and 6 for the unscreened tests. Table 5 shows the critical flotation times along with the total flotation times. Tests C and D presented higher selectivity and lower flotation rates, leading to longer critical times. The flotation protocols in Tests E and F were defined to study the bulk separation of sulphides under high collector dosages, which led to higher mass recoveries and shorter t_{crit}.

Fig. 7a illustrates the incremental ERs in Test C, from which a critical flotation time of 6 min was obtained. Fig. 7b shows the discrete ERs along with the discrete recoveries for the last two flotation times (data labels). The −45 μm, +45–150 μm and +150 μm size-classes were evaluated. The discrete ERs were 2.9 (−45 μm), 12 (+45–150 μm) and 4.6 (+150 μm) at the end of the process with discrete recoveries of 33%, 23% and 12%, respectively. The fine classes showed lower ERs, which were mainly associated with the non-selective separation of gangue (*e.g.* entrainment) and the typically higher feed grades in these fractions. However, these ERs were significantly greater than 1 with non-negligible discrete recoveries in the last flotation interval. The intermediate class showed high discrete ERs, which were always greater than 10 and with a maximum value of 37 at 3 min. The discrete recoveries were in a similar range to those observed in the fine class. The coarse class presented an intermediate condition for the discrete ER, with lower discrete recoveries. The differences in the ERs for the evaluated size classes can be explained by: (i) entrainment of gangue in the finer class, (ii) higher froth selectivity in the coarser classes, (iii) differences in the size-by-size feed grades (−45 μm: 1.1%Cu; +45–150 μm: 1.0%Cu; +150 μm: 0.45%Cu) for similar concentrate grades. The results of Fig. 7b suggest the flotation process was not exhausted and true flotation kept influencing the metallurgical indexes at the end of the experiment. The results of Fig. 7 are also in good agreement with the increasing recoveries presented in Appendix A. It should be noted that Test C showed the highest ERs of the size-by-size tests (Tests C to F), as shown in Table 3, consistently with the results obtained from the discrete analysis. The flotation protocol of Test C can be enhanced by extending the total flotation time, approaching the flotation kinetics to a plateau. This experiment presented only one concentrate after reaching Agar's criterion, which masks the evolution of the discrete ERs and recoveries at the end of the process. Therefore, a flotation time extension or a sampling rate increase allows the kinetic characterization to be improved.

Table 5
Critical flotation times in Tests C to F.

Tests	t_{crit}, min	t_{tot}, min	t_{crit}/t_{tot}, %
C	Cu: 5.0–7.0	12	Cu: 42–59%
D	Pb: 9.2–12 Cu: 9.2–15	32	Pb: 29–39% Cu: 29–46%
E	Cu: 1.0–1.3 Ni: 3.9–4.2	16	Cu: 6.1–7.8% Ni: 25–26%
F	Cu: 2.6 Ni: $t_{crit} > t_{tot}$	7.5	Cu: 34–35% Ni: > 100%

Incremental ERs of Pb are presented in Fig. 8 for Test D. From this curve, a critical flotation time of 10 min was obtained. The discrete ERs at −20 μm, +20–38 μm and +38 μm are also shown in Fig. 8b. The feed grades of Pb (mill product) were 3.3%, 2.0% and 1.8% in these size classes, respectively. Data labels for the discrete recoveries are shown at 24 and 32 min. All the size classes presented decreasing trends for the discrete ERs, with values of 1.7 (−20 μm), 2.2 (+20–38 μm) and 1.7 (+38 μm) in the 24–32 min interval. In addition, the discrete recoveries were R_{-20} = 5.9%, $R_{+20\text{-}38}$ = 1.5% and R_{+38} = 0.4% at the end of the process. The same pattern as Test C was observed for the discrete ERs, with the intermediate class showing the highest ERs and the finest class again presenting the lowest ERs. The results showed that the flotation process was closer to exhaustion than Test C, with significantly lower discrete ER and discrete recoveries in the last flotation interval. However, the discrete ERs were again greater than 1, which implies the contribution of true flotation was still important at the end of the test. The discrete recoveries in the 24–32 min intervals are in good agreement with the kinetic responses of Fig. 2a for long flotation times, with a slightly increasing trend in the −20 μm fraction, and close to steady recoveries in the coarser classes. Appendix C shows the same results for Cu, which presented higher discrete ERs (ER_{-20} = 2.8%, $ER_{+20\text{-}38}$ = 5.8% and ER_{+38} = 5.7%) and higher discrete recoveries (R_{-20} = 10%, $R_{+20\text{-}38}$ = 3.8% and R_{+38} = 1.3%) in the same flotation interval.

Fig. 9 illustrates the results for Ni in Test E under P_{80} = 106 μm, with $t_{crit} \approx 4$ min. The-38 μm, +38–75 μm and +75 μm size-classes were analysed, which presented Ni feed grades of 1.9%, 1.3% and 0.8%, respectively. Test E showed lower selectivity with a mass recovery of 55%. The discrete ERs were $ER_{-38\ \mu m}$ = 1.2, $ER_{+38\text{-}78\ \mu m}$ = 1.0 and $ER_{+75\ \mu m}$ = 0.3 at the end of the process. The fine and intermediate classes presented discrete ERs close to 1 in the 8–16 min interval, which implies the non-selective mechanisms (*i.e.* true flotation of gangue, entrainment and associated gangue) significantly affected the incremental concentrate. For the coarse class, the discrete ER in the 4–16 min interval was significantly lower than 1. This result is also explained by the low selectivity of the process along with the high fraction of valuable minerals in the +150 μm size-class. The contribution of this size fraction to the +75 μm class in each incremental concentrate was lower than 2%. However, 22% of the tailings was in the +150 μm size-class with a grade of 0.6% Ni (and 0.5% Cu). These grades were significantly higher than the tailings grades in the −150 μm class. Although the discrete recoveries were moderately high in the fine and intermediate classes, the low discrete ERs suggest that the contribution of true flotation to the overall recovery is masked by the non-selective separation. The same trends of Fig. 9 were obtained for Cu (with faster flotation kinetics).

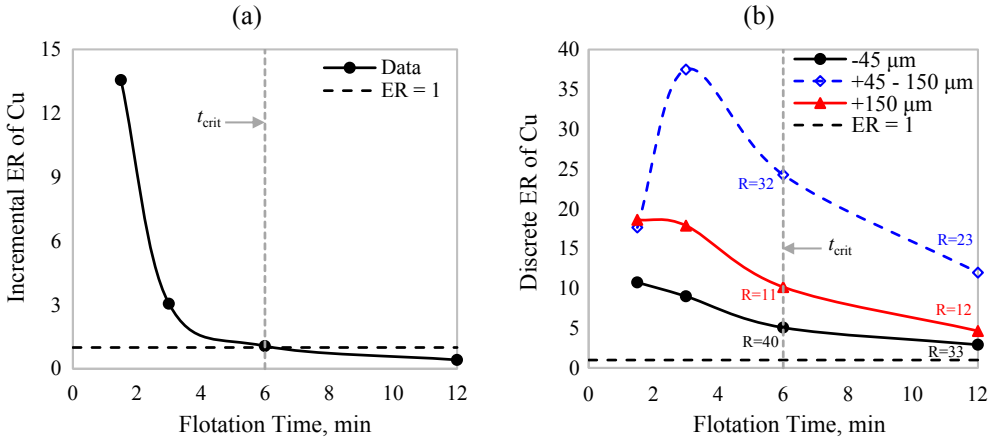

Fig. 7. Test C: (a) incremental ERs of Cu, (b) discrete ERs of Cu size-by-size along with the discrete Cu recoveries (data labels at 6 and 12 min). Trendlines added for visualization purposes only.

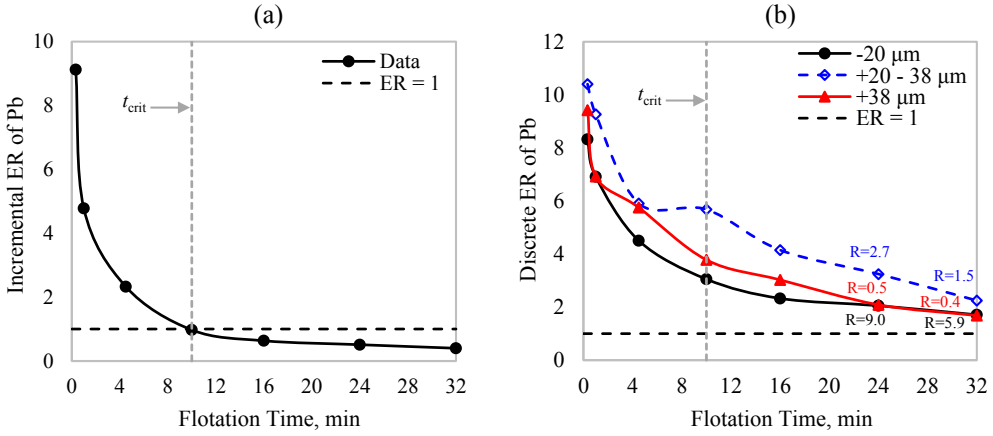

Fig. 8. Test D: (a) incremental ERs of Pb, (b) discrete ERs of Pb size-by-size along with the discrete Pb recoveries (data labels at 24 and 32 min). Trendlines added for visualization purposes only.

Fig. 10 shows the discrete ERs of Ni and Cu in Test E, removing the +150 µm fraction, given its low content in each incremental concentrate. A significant change in the coarser fraction (+75–150 µm) is observed, which became highly correlated with the intermediate class +38–75 µm. The discrete ERs in the +75–150 µm class increased regarding the +75 µm fraction in the 4–16 min interval, reaching values closer to 1 for Ni and Cu. The experimental conditions of Test E favoured the Ni and Cu exhaustion. Thus, close to equilibrium concentrations of these metals were obtained in the flotation cell, leading to discrete ER ≈ 1 at the end of the process. Similar trends to those of Fig. 10 were observed in Test F for the size classes −38 µm, +38–75 µm and +75–106 µm, as shown in Appendix C, with higher ERs and lower flotation rates. It should be noted that the protocols of Tests E and F are uncommon in processes subject to selectivity

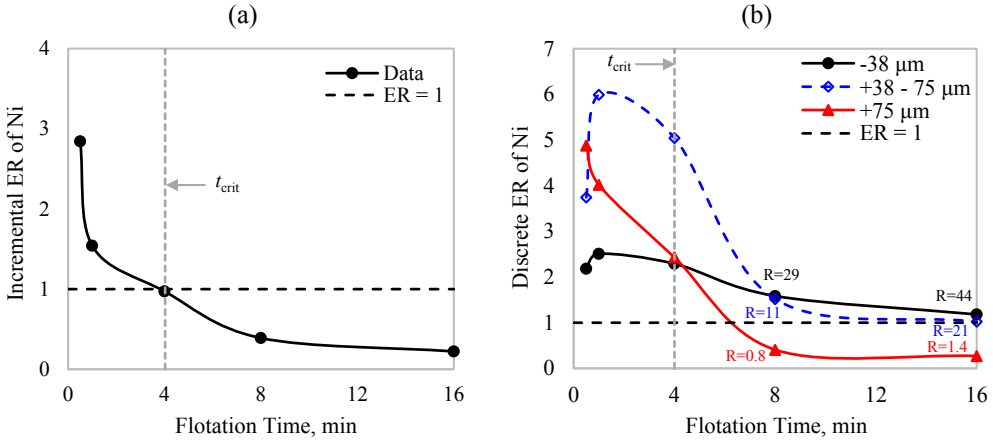

Fig. 9. Test E: (a) incremental ERs of Ni, (b) discrete ERs of Ni size-by-size along with the discrete Ni recoveries (data labels at 8 and 16 min). Trendlines added for visualization purposes only.

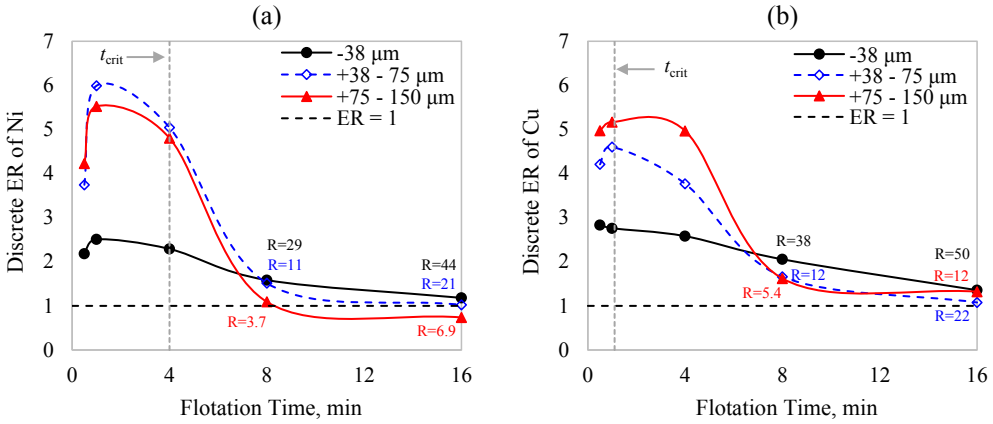

Fig. 10. Test E: discrete ERs size-by-size along with the discrete recoveries at 8 and 16 min (data labels), (a) Ni, (b) Cu. Trendlines added for visualization purposes only.

constraints (*e.g.* upper bounds for the mass recovery, lower bounds for the concentrate grades or specific rejection for some gangue). Thus, trends similar to those of Tests A, B, C and D are expected.

3.4. Discussion

The incremental enrichment ratio and Agar's criterion were applied to different Cu flotation tests. The results showed a good agreement between the measured total recoveries and the estimated maximum recoveries (regression), under flotation times significantly longer than the critical times obtained from Agar's principle.

The flotation tests showed that obtaining discrete ERs < 1 for the valuable metals is not straightforward, even for long flotation times and low-selectivity processes. Some experimental conditions may also present non-negligible discrete recoveries in the last flotation intervals. Therefore, the separation process cannot be considered completely depleted at long flotation times, despite the low incremental recoveries.

The study of the incremental ERs presented here is also applicable at the industrial scale. Discrete ERs $\gg 1$ in the last cell of a flotation circuit can justify the potential for recovery increases. Operating variables that increase the flotation rates (*e.g.*, superficial gas velocity, froth depth, froth discharge velocity) can be manipulated to favour mineral exhaustion.

The discrete ERs were also greater than 1 in almost all the size-by-size experiments, except for Test E, which showed low selectivity and high flotation rates. Non-selective processes commonly define the mass recoveries for $t \rightarrow \infty$ because of entrainment of fine particles. However, even the finer classes presented ER > 1 at long flotation times. This result contradicts the assumption that valuables are recovered by entrainment at the end of the tests.

In summary, a level of exhaustion that guarantees discrete ERs close to 1, for long flotation times (non-selective separation), can be only obtained under specific experimental conditions. In addition, the low incremental recoveries commonly observed at the end of the batch processes cannot be only attributed to the non-selective recovery of valuable metals.

4. Conclusions

Six different batch flotation protocols were used to study the incremental and discrete enrichment ratios along the laboratory tests. The former index was employed along with Agar's criterion to evaluate the agreement between the total measured recovery and the maximum recovery estimated by regression. Both parameters were more consistent when critical flotation times t_{crit} lower than 40% of the total flotation time were utilized. Thus, curves of incremental ER versus time along with typical t_{crit} values can be used to define the total flotation times at laboratory scale.

Discrete ERs significantly greater than 1 were observed in processes close to exhaustion. In addition, discrete recoveries may be significant even though the cumulative recoveries as a function of time approach a plateau. Thus, further analyses of the laboratory data are required to evaluate the process depletion.

Four size-by-size tests were studied to determine the distribution of the discrete enrichment ratios at the end of the processes. All the size-classes presented discrete ERs greater than 1 at long flotation times, except for one condition subject to fast kinetic response, high mass recovery, moderately long flotation time and high content of non-floatable valuable mineral in the coarsest class. Therefore, although the non-selective mechanisms (*e.g.*, entrainment, true flotation of gangue and gangue association) predominantly influence the mass recovery in the last flotation intervals, the contribution of true flotation to the overall discrete recoveries cannot be considered negligible in processes with low feed grades and subject to selectivity constraints.

Acknowledgements

The authors are grateful for the financial support from the Natural Sciences and Engineering Research Council of Canada (NSERC), Teck Resources Ltd., COREM, SGS Canada Inc., and ChemIQA, under the Collaborative Research and Development Grants Program (CRDPJ 531957 - 18). The McGill Engineering Doctoral Award (MEDA) from the Faculty of Engineering at McGill University is also acknowledged for providing funding for L. Vinnett and C. Marion. C. Marion also acknowledges funding from the NSERC Alexander Graham Bell Canada Graduate Scholarships Program.

Appendix A

Fig. A1 shows the size-by-size kinetic responses in Tests C and F. Similar trends to those obtained in Tests D and E were observed for the flotation kinetics in equivalent size-classes. The mass recoveries were 18% and 55% in Tests C and F, respectively.

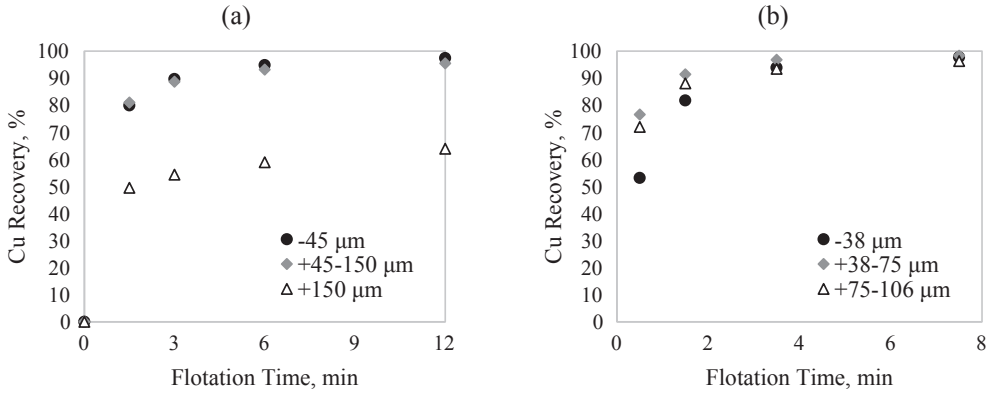

Fig. A1. Recovery as a function of time for different size classes: (a) Cu kinetics, Test C, P_{80} = 150 µm; (b) Cu kinetics, Test F, P_{80} = 63 µm.

Appendix B

Enrichment ratios

Kinetic responses in flotation are obtained from recovery estimates as a function of time. Eq. (B.1) describes the recovery of a component for a given flotation time $R(t)$:

$$R(t) = \left[\frac{x_C(t)}{x_F}\right]\cdot\left[\frac{C(t)}{F}\right] = ER(t)\cdot w(t) \quad \text{(B.1)}$$

where x_F corresponds to the feed grade, F to the initial mass in the feed and $x_C(t)$ and $C(t)$ are the cumulative concentrate grade and concentrate mass, respectively. The values of $x_C(t)$ and $C(t)$ are obtained from the total solids recovered in the interval $[0, t]$. In Eq. (B.1), $ER(t) = x_C(t)/x_F$ and $w(t)$ are the cumulative enrichment ratio and the cumulative mass recovery, respectively. In continuous operation, Eq. (B.1) is applied as a function of the residence time or the machine number along a flotation circuit.

The definition of ER in Eq. (B.1) can be generalized to obtain the incremental ER as the incremental concentrate grade divided by the overall feed grade (Agar et al., 1980; Jowett and Sutherland, 1985). In an arrangement of flotation machines in series, the incremental concentrate grade corresponds to the concentrate grade in the n-th cell, whereas in a batch process corresponds to the concentrate grade in a specific flotation interval.

Similarly, for an arrangement of flotation machines in series, the ER in the n-th cell is defined as the ratio between the concentrate and feed grades in that specific cell. In a batch process, this discrete parameter can be estimated from the ratio between an incremental concentrate grade and the grade of the material that is processed in the evaluated flotation interval. This discrete ER approximates the instantaneous ER. The same approach can be used to define a discrete recovery, using as a reference the material that is in the cell prior to the flotation interval.

Appendix C

Fig. C1(a) shows the incremental ERs of Cu in Test D, from which a critical flotation time of 10 min was determined. Fig. C1(b) shows the discrete ERs of Cu at −20 µm (x_F = 1.0%Cu), +20–38 µm (x_F = 0.9%Cu) and +38 µm (x_F = 0.9%Cu). Data labels for the discrete recoveries are shown at 24 and 32 min. The discrete ER were 2.8 (-20 µm), 5.7 (+20–38 µm) and 5.8 (+38 µm) with discrete recoveries of R_{-20} = 10%, $R_{+20\text{-}38}$ = 3.8% and R_{+38} = 1.3% in the last flotation interval. The finer class presented lower discrete ERs, whereas the two coarser classes kept the same range for this ER. All the discrete ERs were significantly greater than 1 and greater than the discrete ERs of Pb.

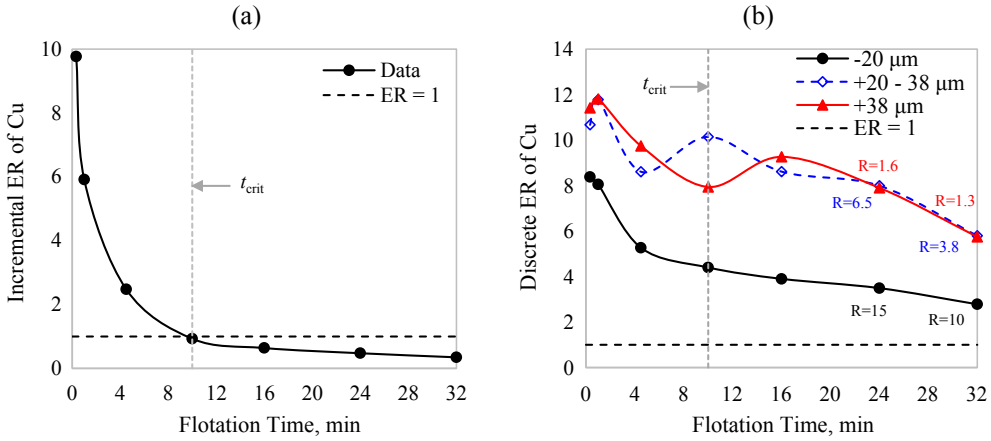

Fig. C1. Test D: (a) incremental ERs of Cu, (b) discrete ERs of Cu size-by-size along with the discrete Cu recoveries (data labels at 24 and 32 min). Trendlines added for visualization purposes only.

Appendix D

The incremental ERs of Cu in Test F are presented in Fig. D1(a). A critical flotation time of 2.6 min is observed. The discrete ERs of Cu at −38 μm, +38–75 μm and +75–106 μm are also shown in Fig. D1(b) along with the discrete recoveries at 3.5 and 7.5 min (data labels). The discrete ERs were 1.8 (−38 μm), 1.8 (+38–75 μm) and 2.9 (+75–106 μm) with significant discrete recoveries of R_{-38} = 63%, R_{+38-75} = 47% and R_{+75} = 44% in the last flotation interval. Test F showed similar patterns as Test E removing the class + 150 μm. However, lower recovery rates and higher ERs were observed in Test F, which is in good agreement with the t_{crit} values presented in Table 5.

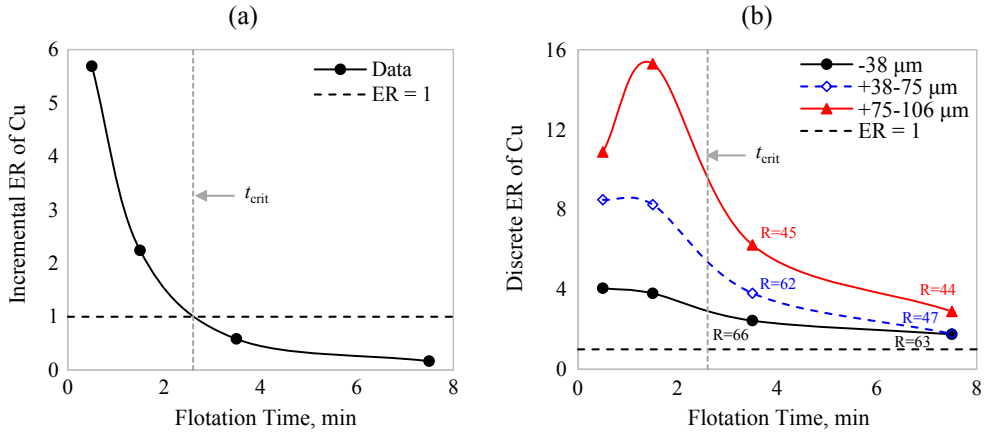

Fig. D1. Test F: (a) incremental ERs of Cu, (b) discrete ERs of Cu size-by-size along with the discrete Cu recoveries (data labels at 3.5 and 7.5 min). Trendlines added for visualization purposes only.

References

Agante, E., Carvalho, T., Durão, F., Pinto, A., Mariano, T., 2007. Kinetic study of froth flotation for PET-PVC separation, 2004 new and renewable energy technologies for sustainable development. Evora 117–126.

Agar, G.E., Stratton-Crawley, R., Bruce, T.J., 1980. Optimizing the design of flotation circuits. Canad. Min. Metall. Bull. 73, 173–181.

Carrasco, C., 2010. Modelación Zona de Colección y Espuma para Supervisión y Control Industrial. Federico Santa María Technical University, Valparaíso, Chile, Department of Chemical and Environmental Engineering.

Celik, I.B., 2015. Mineralogical interpretation of the collector dosage change on the sphalerite flotation performance. Int. J. Miner. Process. 135, 11–19.

Garcia-Zuñiga, H., 1935. La recuperación por flotación es una función exponencial del tiempo. Boletín Minero, Sociedad Nacional de Minería 47, 83–86.

Girard, M., Hodouin, D., Bazin, C., 2005. Ability of kinetic flotation models to simulate interactions between grinding and flotation. Can. Metall. Q. 44, 379–392.

Hadler, K., 2015. The link between froth surface grade and flotation feed grade. Miner. Eng. 78, 32–37.

Harris, C., Chakravarti, A., 1970. Semi-batch froth flotation kinetics: species distribution analysis. Transac. AIME 247, 162–172.

Hay, M.P., 2008. Optimising froth condition and recovery for a nickel ore. Miner. Eng. 21, 861–872.

Imaizumi, T., Inoue, T., 1963. Kinetic consideration of froth flotation. In: Roberts, A. (Ed.), Sixth International Mineral Processing Congress. Pergamon Press, Cannes, pp. 581–593.

Jowett, A., 1975. Formulae for the technical efficiency of mineral separations. Int. J. Miner. Process. 2, 287–301.

Jowett, A., Sutherland, D.N., 1985. Some theoretical aspects of optimizing complex mineral separation systems. Int. J. Miner. Process. 14, 85–109.

Kelsall, D.F., 1961. Application of probability assessment of flotation systems. Transac. Instit. Min. Metall. 70, 191–204.

King, R.P., 2012. Flotation, in: Schneider, C.L., King, R.P. (Eds.), Modeling and simulation of mineral processing systems, 2nd ed. Society for Mining, Metallurgy, and Exploration, Inc., USA, pp. 341-416.

Maldonado, M., Araya, R., Finch, J., 2011. Optimizing flotation bank performance by recovery profiling. Miner. Eng. 24, 939–943.

Mohammadi-Jam, S., 2017. An Investigation Into the Applicability of Inverse Gas Chromatography to Mineral Flotation. McGill University, Montreal, Department of Mining and Materials Engineering.

Ramlall, N.V., 2013. An Investigation Into the Effects of UG2 Ore Variability on Froth Flotation. University of KwaZulu-Natal, Durban.

Ramlall, N.V., Loveday, B.K., 2015. A comparison of models for the recovery of minerals in a UG2 platinum ore by batch flotation. J. South Afr. Inst. Min. Metall. 115, 221–228.

Ross, V.E., 1990. Flotation and entrainment of particles during batch flotation tests. Miner. Eng. 3, 245–256.

Runge, K., 2010. Laboratory flotation testing–an essential tool for ore characterisation. Flotation plant optimisation a metallurgical guide to identifying and solving problems in flotation plants. Spectrum Series 155–173.

Savassi, O.N., 2006. Estimating the recovery of size-liberation classes in industrial flotation cells: a simple technique for minimizing the propagation of the experimental error. Int. J. Miner. Process. 78, 85–92.

Seguel, F., Soto, I., Krommenacker, N., Maldonado, M., Becerra Yoma, N., 2015. Optimizing flotation bank performance through froth depth profiling: Revisited. Miner. Eng. 77, 179–184.

Sutherland, D.N., 1989. Batch flotation behaviour of composite particles. Miner. Eng. 2, 351–367.

Trahar, W.J., Warren, L.J., 1976. The flotability of very fine particles—a review. Int. J. Miner. Process. 3, 103–131.

Vinnett, L., Alvarez-Silva, M., Jaques, A., Hinojosa, F., Yianatos, J., 2015. Batch flotation kinetics: fractional calculus approach. Miner. Eng. 77, 167–171.

Vinnett, L., Navarra, A., Waters, K.E., 2019. Comparison of different methodologies to estimate the flotation rate distribution. Miner. Eng. 130, 67–75.

Yianatos, J., Bergh, L., Vinnett, L., Panire, I., Iriarte, V., 2016. Correlation between the top of froth grade and the operational variables in rougher flotation circuits. Miner. Eng. 99, 151–157.

Yianatos, J., Bergh, L., Vinnett, L., Rojas, I., 2014. On the collection of valuable minerals along rougher flotation banks. Miner. Eng. 66–68, 202–206.

Yianatos, J., Henriquez, F., Oroz, A., 2006. Characterization of large size flotation cells. Miner. Eng. 19, 531–538.

Zanin, M., Wightman, E., Grano, S.R., Franzidis, J.P., 2009. Quantifying contributions to froth stability in porphyry copper plants. Int. J. Miner. Process. 91, 19–27.